Transactions of the Materials Research Society of Japan 29[4] 1249-1252 (2004)

Effect of post-annealing on superconductive properties of dip-coated Bi-2223 tapes

Masaki Sumida, Akiyoshi Matsumoto, Petre Badica and Hiroaki Kumakura
National Institute for Materials Science (NIMS), Superconducting Materials Center,
1-2-1 Sengen, Tsukuba, Ibaraki 305-0047, Japan
Fax: 81-859-2301, e-mail: sumida.masaki@nims.go.jp

In this report, effect of post-annealing on the superconductive properties of the high T_c superconductive Bi-2223/Ag tapes was studied. Monocore tapes were prepared by the dip-coating method, and the thermo-mechanical process was applied to them in air. This process includes a final heat treatment with an isothermal post-annealing. After an isotherm at 836°C for 48 h, successive isotherms were applied at extensively varied temperatures in a range of 820-400°C at a fixed time of 12h. Two peaks were observed against this temperature in the critical current density (J_c) at 77 K as well as in the critical temperature (T_c). These were measured by the four probe method along with 1μV/cm criterion and the AC susceptibility measurements, respectively. The phase formation behavior and microstructure development were identified from XRD and SEM-EDS analyses. A qualitative understanding was obtained with the aid of the reported equilibrium phase relationships and it could be correlated with the results of the J_c and T_c. Furthermore, stepwise post-annealing process was applied to the same tapes. Post-annealing of two sequential isotherms was conducted by adopting the two peak temperatures found above. Optimizing the isothermal temperature and time, the enhanced J_c was obtained relative to that by normal post-annealing.
Key words: Bi-2223, superconductor, post-annealing, J_c

1. INTRODUCTION

The microstructure control is a crucial technique to improve the superconductive properties of the high T_c Bi-2223 ($Bi_2Sr_2Ca_2Cu_3O_x$) cables and wires. Enhancement in the bulk density, grain alignment and connectivity, phase purity, oxygen content, and elimination of second phase particles and microcracks are principal goal for that. By this technique, suppression of the weak link characteristics and introduction of the pinning centers into the microstructure would be realized. The critical current density J_c can be improved by them, which is decisively important to arrive at industrial applications in the field of power, electronics, communication, and medical and other technologies.

Two-step heat treatment has been developed for PIT-processed Bi-2223 tapes. This process consists of two successive isotherms at different temperatures. Liu et al.[1] varied the second isothermal temperature within 700-845°C after the first isotherm at 841°C and observed a maximum in J_c and Bi-2223 phase fraction at 825°C. This result shows the significance of post-annealing. However, the phase and microstructure formation mechanism and their effects on J_c have not yet been fully understood.

In this report, the phase formation and superconductive properties of dip-coated Bi-2223 tapes are studied by post-annealing at an extensively wide range of temperature. It is shown that the J_c and T_c highly depend on this temperature, and two peaks were observed in both the J_c and T_c. By means of phase identification, microscopic observation and quantitative analysis, the phase and microstructure formation and its effect on the properties are discussed with the aid of the reported equilibrium phase relationships. Furthermore, taking the temperatures at the peaks, stepwise post-annealing was developed for the same tapes. Optimizing the heating condition, this process yielded the enhanced J_c relative to that by the normal post-annealing.

2. EXPERIMENTAL

Commercial powder with a nominal composition of $Bi_{1.88}Pb_{0.33}Sr_{2.00}Ca_{1.97}Cu_{3.00}O_x$ (Dowa co., ~2 μm) was used for the starting material. Ag-clad monocore tapes were prepared by the dip-coating for the thermo-mechanical process. The entire process was completed in air. Tapes of approximately 200 μm in thickness with an oxide core of 40-45 μm in thickness were first roll-pressed to reduce their thickness to 170 μm. The first heat treatment was made for them at T_1=842 °C for t_1=96 h in a box furnace with furnace cooling. Heating profile in this process is drawn in Fig. 1(a). After this treatment, tapes expanded its thickness slightly. The second roll pressing was made to reduce the thickness to 90 μm. Tape preparation process can be found in detail elsewhere[2,3].

Subsequently, the second heat treatment was made in a horizontal tube furnace. The temperature history in this process is illustrated in Fig. 1(b). After the initial isotherm, isothermal post-annealing was conducted in succession, taking a form of two-step profile. Here $T_1^{(2)}$

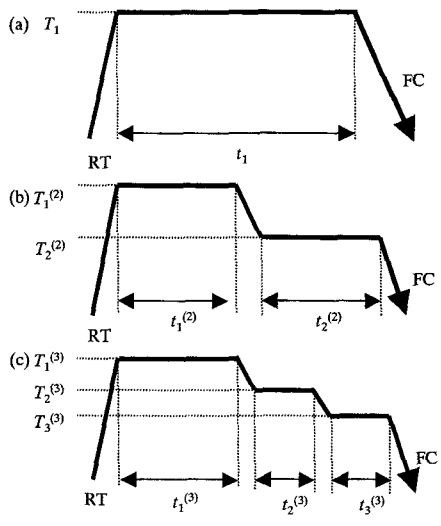

Fig. 1 Heat treatment processes in (a) the first heat treatment, (b) the second heat treatment with single post-annealing and (c) heat treatment with stepwise post-annealing.

and $t_1^{(2)}$ were chosen as $T_1^{(2)}$=836°C and $t_1^{(2)}$=48 h. For the post-annealing, extensively different $T_2^{(2)}$ in a range of 820-400°C was applied under a fixed condition at $t_2^{(2)}$=12h. Also, $t_2^{(2)}$ was varied up to 192h at $T_2^{(2)}$= 810°C. For reference purposes, some tapes undertook a simple isothermal heat treatment at 836°C and 48 h with no post-annealing to enable a comparison with above.

Furthermore, stepwise post-annealing was developed for the same tapes. This process contains sequential isotherms at two different temperatures that take the form of a three-step profile. The heating profile in this process is illustrated in Fig. 1(c), and it is applied to the tapes instead the two-step. The peak temperatures found in the two-step results were taken into one process. $T_1^{(3)}$ and $t_1^{(3)}$ were taken to be the same as $T_1^{(2)}$ and $t_1^{(2)}$, respectively. $T_2^{(3)}$ =810°C for $t_2^{(3)}$ =12h were chosen and several different $T_3^{(3)}$ in a range of 700-500°C were examined at $t_3^{(3)}$=12h. Furnace cooling is adopted between these isotherms.

Microstructure observation and quantitative analysis were made with scanning electron microscopy (SEM-EDS) on the polished cross section of the tapes. X-ray diffraction (XRD) with Cu target was used for phase identification. The transport J_c measurements were made by the four-probe method at the liquid nitrogen temperature in the self-field along with 1 μV/cm criterion. At least three tapes were provided so that the scattering of the measured values could be evaluated. The onset T_c was estimated from AC susceptibility measurements in which the measurement error was assumed to be within 1 K.

3. RESULTS

Figure 2 shows the J_c as a function of $T_2^{(2)}$. This figure shows that the J_c is highly dependent on $T_2^{(2)}$. Two peaks are observed in this figure. A sharp peak is found at $T_2^{(2)}$=810°C. Another broad peak is found at $T_2^{(2)}$=600-660°C. Within $T_2^{(2)}$=700-800°C, the J_c

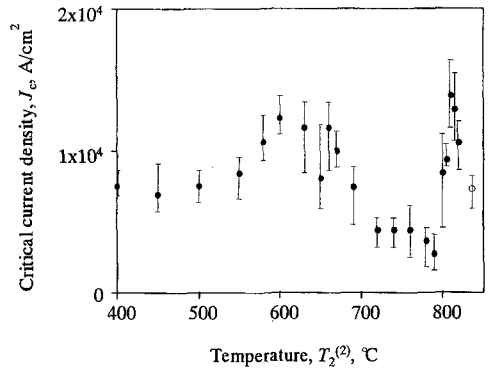

Fig. 2 The J_c at 77 K of Bi-2223 tapes as a function of $T_2^{(2)}$ in post-annealing. Mean value and error width with the maximum and the minimum in measurements are plotted. Open circles indicate a reference processed with no post-annealing.

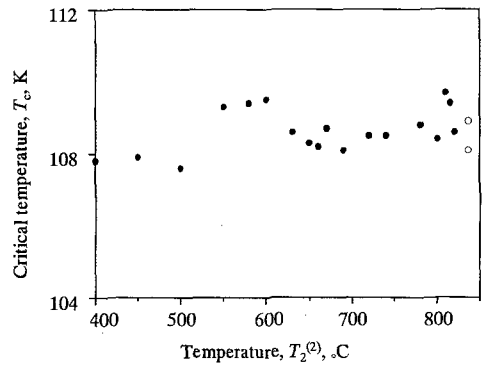

Fig. 3 The T_c of Bi-2223 tapes as a function of $T_2^{(2)}$ in post-annealing. Open circles indicate a reference processed with no post-annealing.

degraded, and, below 600°C a substantial decrease was also observed. The J_c of the reference sample is plotted with open circles. It is shown that the J_c can be enhanced by post-annealing at appropriate $T_2^{(2)}$ relative to that by no post-annealing. Figure 3 shows the T_c as a function of $T_2^{(2)}$. The T_c also shows two peaks. There are a sharp peak at $T_2^{(2)}$=810°C with T_c=109.7 K and a broad one is at $T_2^{(2)}$=550-600°C with T_c=109.3-109.5K. The latter, however, does not completely cover that of the J_c and is 50-60K lower. The reference T_c is plotted with open circles in this figure, where two different measurements on samples processed under the same condition show a difference in T_c of 0.8K. However, this figure shows significant enhancement in T_c by post-annealing at appropriate $T_2^{(2)}$.

Figure 4 shows SEM microphotographs in cross sections of several different $T_2^{(2)}$ along with the reference. They show that the microstructure is mainly composed of dense Bi-2223 particles in all of the temperatures. From general observation and comparison with the reference in Fig. 4(a), coarse particles stand out in the microstructure above $T_2^{(2)}$=720°C, and very few particles were found below $T_2^{(2)}$=670°C. The arrows in Fig. 4(b)-(c) indicate the particles. From XRD and quantitative analyses, most of them were identified to be $(Ca,Sr)_2PbO_4$. Very coarse particles were observed in

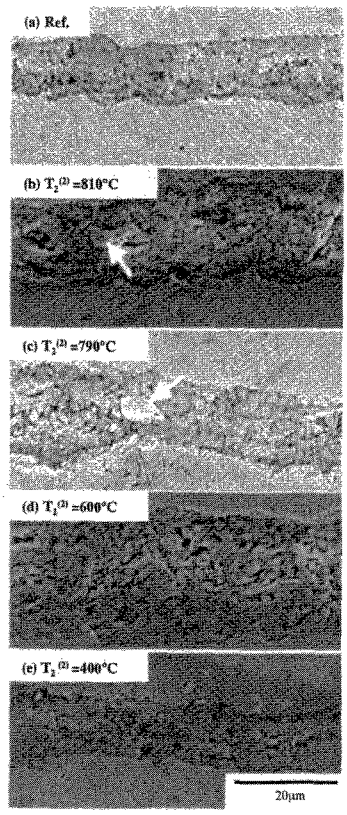

Fig. 4 SEM microphotographs of oxide cores in Bi-2223 tapes as a function of $T_2^{(2)}$ in post-annealing, (a) a reference, (b)$T_2^{(2)}$=810°C, (c)790°C, (d)600°C and (e)400°C.

the microstructure of long second isotherm at $T_2^{(2)}$=810°C for $t_2^{(2)}$=192h, as shown in the center of Fig. 5. Figure 6 shows XRD results of the reference, $T_2^{(2)}$=800°C and 400°C. This figure shows that the Bi-2223 and Bi-2212 are principal, and residual $(Ca,Sr)_2PbO_4$, $Sr_{14}Ca_{24}O_{41}$ and 3221 are clearly observed at 800°C. These figures show that these are stable phases at this temperature range and coarsen during the isotherm. Figure 7 shows $t_2^{(2)}$ dependence on J_c at $T_2^{(2)}$=810°C. The J_c increases with $t_2^{(2)}$ up to 12h then decreases. This figure shows that long post-annealing degrades the J_c, that is caused by the coarse particles.

Figure 8 shows the result of stepwise post-annealing on the J_c as a function of $T_3^{(3)}$. This figure shows that the J_c is largely dependent on $T_3^{(3)}$. The optimum $T_3^{(3)}$ is found at 600°C. This figure proves that this process can yield even better J_c than those shown in Fig. 2.

4. DISCUSSION

Both Figs. 2 and 3 contain sharp and broad peaks at high and low temperatures respectively. The high peak is located at $T_2^{(2)}$=810°C. The low one is located at $T_2^{(2)}$=600-660°C in J_c and 550-600°C in T_c. Liu et al.[1] observed a similar peak in J_c at 825°C on PIT-processed Bi-2223. They described that the Bi-2223 phase fraction is maximized at this temperature and that this is the lowest temperature at which liquid forms while Bi-2201 is removed from grain boundaries. Phase and microstructure formation at different post-annealing

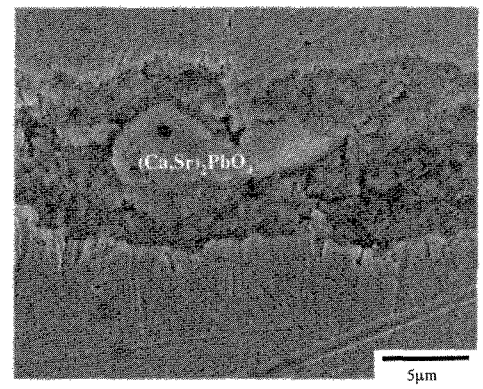

Fig. 5 SEM microphotograph of an oxide core in Bi-2223 tape post-annealed at $T_2^{(2)}$=810°C for $t_2^{(2)}$=192h.

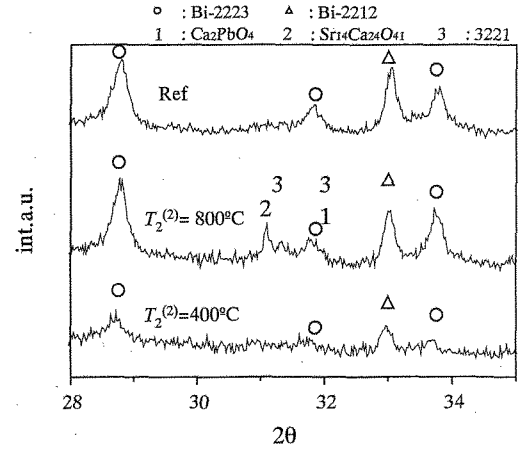

Fig. 6 XRD patterns between 28-35° of Bi-2223 tapes of the reference, $T_2^{(2)}$=800°C and 400°C.

temperature can be explained qualitatively with the aid of equilibrium phase diagrams. The equilibrium Pb content in the Bi-2223 phase is maximum at 850°C and decreases with a decrease in temperature, and the Bi-2223 phase can contain almost no Pb at 750°C[4,5]. The solid solubility limit is highly dependent on the temperature. The Bi-2223 single phase is stable above this limit. Below the limit, there is a multi-phase region, where Bi-2223 with Bi-2212, Ca_2PbO_4, 3221, CuO, and Ca_2CuO_3 are stable. $Sr_{14}Cu_{24}O_{41}$ may appear at a low Pb composition. This equilibrium boundary would be at 820-830°C for the nominal composition.

Assuming that Bi-2223 is at equilibrium in Pb content by post-annealing, the Pb content in Bi-2223 decreases, and more Pb is released from Bi-2223 with a decrease in $T_2^{(2)}$. Released Pb should contribute to the formation of secondary particles. Thus the Bi-2223 phase fraction should decrease. The Pb content might take the optimum value for the T_c at $T_2^{(2)}$=810°C and consequently for the J_c, even though the microstructure contains secondary particles.

On cooling into the multi-phase region, Bi-2223 decomposes, and other phases grow kinetically. In principle, the system approaches to equilibrium phase fraction and microstructure during an isotherm. Figures 4(b), 5 and 6 can be evidence that $T_2^{(2)}$=810°C is within

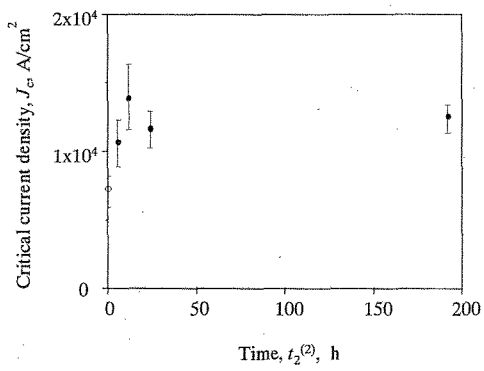

Fig. 7 The J_c at 77 K of Bi-2223 tapes as a function of $t_2^{(2)}$ in post-annealing at $T_2^{(2)}$=810°C. Mean value and error width with the maximum and the minimum in measurements are plotted. Open circles indicate a reference processed with no post-annealing.

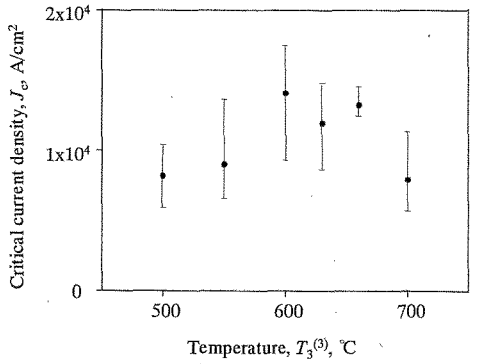

Fig. 8 The J_c at 77K of Bi-2223 tapes as a function of $T_3^{(3)}$ in stepwise post-annealing. Mean value and error width with the maximum and the minimum in measurements are plotted.

this multi-phase region. However, the post-annealing at this temperature should improve the grain growth and connectivity without a significant decomposition of Bi-2223. The long isotherm, meanwhile, yields particle coarsening and also Bi-2223 decomposition, which lowers the J_c as shown in Fig. 7. Phase transformation kinetics accelerates with an increase in undercooling from the equilibrium limit, as long as the rate constant does not decrease significantly due to the temperature decrease. Below 810°C, Bi-2223 decomposes, and secondary phase particles grow substantially. The refined microstructure for the J_c is obtained only under appropriate temperature and time.

Figure 4 (d)-(e) shows that coarse particles are not observed at this temperature range that is within and also below the broad peaks. The microstructure can be refined but does not dominate the properties here. The Bi-2223 is non-stoichiometric in oxygen, and its equilibrium content is a function of the temperature and oxygen partial pressure[6]. Under an air atmosphere, the oxygen content is largely temperature dependent above 700°C but less sensitive to the temperature within 600-200°C. The higher T_c is revealed with a larger oxygen content, which can be achieved at low temperature. The broad peak in T_c at $T_2^{(2)}$=550-600°C in Fig. 3 is caused by the increment in the oxygen content. An optimum amount of oxygen might be introduced into Bi-2223 at this temperature. The J_c is consequently enhanced due to maximization of the current carrying capacity. However, probable overdoping in oxygen may contribute to their decrements below this temperature. The discrepancy in the temperature range of broad peaks in J_c and T_c should be caused by the non-equilibrium microstructural behavior during post-annealing. That is, relatively short time annealing does not significantly improve the grain growth and connectivity, particularly in a low temperature range. Since the T_c depends less on the microstructure, a broad peak temperature range in J_c would shift to a lower temperature and tend to coincide with that in T_c under longer annealing.

As shown in Fig. 8, stepwise post-annealing is an efficient process to yield high J_c. This process can realize Bi-2223 phase formation, improvement in grain growth and connectivity, and optimization of Pb and oxygen content in one process. The optimum $T_3^{(3)}$ is found at 600°C, a temperature that coincides with the second peak in Figures 2 and 3. This result can be a proposal of a potentially interesting heat treatment process with industrial significance.

5. SUMMARY

Adopting a different post-annealing condition, phase formation and superconductive properties were studied on the Bi-2223/Ag tapes prepared by dip-coating method. The post-annealing temperature, $T_2^{(2)}$, was varied extensively. Two peaks were found both in J_c and T_c. From phase identification, microstructure observation and quantitative analysis, the former peak can be explained from the Bi-2223 single phase stability limit. Enhancement in grain growth and connectivity and Pb reduction can contribute to it. Below this temperature and with long isotherm at this temperature, Bi-2223 decomposition and secondary particle formation prevail and lead to degradation of the microstructure. The latter peak is due to oxygen doping.

Taking on the two peaks in $T_2^{(2)}$, stepwise post-annealing was proposed and applied to the same tapes. Several different third isothermal temperatures, $T_3^{(3)}$, were examined. The optimum for the J_c was found at $T_3^{(3)}$=600°C. The Bi-2223 phase formation, grain growth and connectivity, and optimization of Pb and oxygen content combine into one process and contribute to enhance the J_c.

REFERENCES

[1] H.K. Liu, R. Zeng, X.K. Fu and S.X. Dou, Physica C **325** 70 (1999)
[2] M. Sumida, A. Matsumoto and H. Kumakura, Mater. Trans. JIM, 44 9 (2003) 1872-1876
[3] M. Sumida, H. Kumakura and A. Matsumoto, Supercond. Sci. Tech., in press
[4] P. Majewski, S. Kaesche and F. Aldinger, J. Am. Ceram. Soc. **80** (5) 1174 (1997)
[5] P. Majewski, J. Mater. Res. **15** 854 (2000)
[6] Y. Idemoto, S. Ichikawa and K. Fueki, Physica C **181** 171 (1991)

(Received October 13, 2003; Accepted March 5, 2004)